International Journal of Engineering, Mathematical and Physical Sciences
ISSN: 2517-9934
Vol:7, No:12, 2013

Unsteady Heat and Mass Transfer in MHD Flow of Nanofluids over Stretching Sheet with a Non-Uniform Heat Source/Sink

Bandaris Shankar, Yohannes Yirga

***Abstract*—**In this paper, the problem of heat and mass transfer in unsteady MHD boundary-layer flow of nanofluids over stretching sheet with a non uniform heat source/sink is considered. The unsteadiness in the flow and temperature is caused by the time-dependent stretching velocity and surface temperature. The unsteady boundary layer equations are transformed to a system of non-linear ordinary differential equations and solved numerically using Keller box method. The velocity, temperature, and concentration profiles were obtained and utilized to compute the skin-friction coefficient, local Nusselt number, and local Sherwood number for different values of the governing parameters viz. solid volume fraction parameter, unsteadiness parameter, magnetic field parameter, Schmidt number, space-dependent and temperature-dependent parameters for heat source/sink. A comparison of the numerical results of the present study with previously published data revealed an excellent agreement.

***Keywords*—**Manetohydrodynamics, nanofluid, non-uniform heat source/sink, unsteady.

I. Introduction

THE study of boundary layer flow of an electrically conducting fluid has many applications in manufacturing and natural process which include cooling of electronic devices by fans, cooling of nuclear reactors during emergency shutdown, cooling of an infinite metallic plate in a cooling bath, textile and paper industries, glass-fiber production, manufacture of plastic and rubber sheets, the utilization of geothermal energy, the boundary layer control in the field of aerodynamics, food processing, plasma studies and in the flow of biological fluids.

Magnetohydrodynamics (MHD) is the study of the flow of electrically conducting fluids in a magnetic field. Many experimental and theoretical studies on conventional electrically conducting fluids indicate that magnetic field markedly changes their transport and heat transfer characteristics.

The unsteady boundary layer flow over a stretching sheet has been studied by Devi et al. [1], Elbashbeshy and Bazid [2], Tsai et al. [3] and Ishak [4].

Fluid heating and cooling are important in many industries such as power, manufacturing, transportation, and electronics. Effective cooling techniques are greatly needed for cooling any sort of high-energy device. Common heat transfer fluids such as water, ethylene glycol, and engine oil have limited/poor heat transfer capabilities due to their low heat transfer properties. In contrast, metals have thermal conductivities up to three times higher than these fluids, so it is natural that it would be desired to combine the two substances to produce a heat transfer medium that behaves like a fluid, but has the thermal conductivity of a metal. A lot of experimental and theoretical researches have been made to improve the thermal conductivity of these fluids. In 1993, during an investigation of new coolants and cooling technologies at Argonne national laboratory in U.S, Choi invented a new type of fluid called Nanofluid [5]. Nanofluids are fluids that contain small volumetric quantities of nanometer-sized particles, called nanoparticles. The nanoparticles used in nanofluids are typically made of metals (Al, Cu, Ag, Au, Fe), oxides (Al_2O_3, CuO, TiO_2), metal carbides (SiC), nonmetals (graphite carbon nanotubes), nitrides (AlN, SiN), and others. Common base fluids include water, ethylene glycol and oil. Nanofluids commonly contain up to a 5% volume fraction of nanoparticles to see effective heat transfer enhancements. Nanofluids are studied because of their heat transfer properties: they enhance the thermal conductivity and convective properties over the properties of the base fluid. Moreover, the presence of the nanoparticles enhance the electrical conductivity property of the nanofluids, hence are more susceptible to the influence of magnetic field than the conventional base fluids. The suspended metallic or nonmetallic nanoparticles change the transport properties and heat transfer characteristics of the base fluid, hence enhance the heat transfer of the base fluid. Typical thermal conductivity enhancements are in the range of 15-40% over the base fluid and heat transfer coefficient enhancements have been found up to 40% [6].

Nanofluids have enhanced thermophysical properties such as thermal conductivity, thermal diffusivity, viscosity and convective heat transfer coefficients compared to those of base fluids. Thermophysical properties of nanofluids have been studied by, among others, Kang et al. [7], Velagapudi et al. [8] and Rudyak et al. [9].

After the pioneer investigation of Choi, thriving experimental and theoretical researches were undertaken to discover and understand the mechanisms of heat transfer in nanofluids. The knowledge of the physical mechanisms of heat transfer in nanofluids is of vital importance as it will

B. Shankar, Prof., is with department of Mathematics, Osmania University, Hyderabad, AP, 500007, Inida (phone: +91-9346347026; fax: +91-4027090020; e-mail: bandarishanker@yahoo.co.in).

Y. Yohannes is with Osmania University, Hyderabad, AP, 500007 India (phone: +91-8801070897; fax: +91-4027090020; e-mail: yoahannesalbin@yahoo.com).

enable the exploitation of their full heat transfer potential. Masuda et al. [10] observed the characteristic feature of nanofluid is thermal conductivity enhancement. This observation suggests the possibility of using nanofluids in advanced nuclear systems [11]. A comprehensive survey of convective transport in nanofluids was made by Buongiorno [12], who says that a satisfactory explanation for the abnormal increase of the thermal conductivity and viscosity is yet to be found. He focused on further heat transfer enhancement observed in convective situations. Khan and Pop [13] presented a similarity solution for the free convection boundary layer flow past a horizontal flat plate embedded in a porous medium filled with a nanofluid. Makinde and Aziz [14] studied MHD mixed convection from a vertical plate embedded in a porous medium with a convective boundary condition.

The interaction of magnetic field with nanofluids have several potential applications and may be used to deal with problems such as cooling of nuclear reactors by liquid sodium and induction flow meter which depends on the potential difference in the fluid in the direction perpendicular to the motion and to the magnetic field [15]. During chemotherapy failure to provide localized drug targeting, results in an increase of toxic effects on neighboring organs and tissues, this is precisely done by magnetic drug targeting. This technology is based on binding established anticancer drugs with magnetic nanoparticles (ferrofluids) that concentrate the drug in the area of interest (tumor site) by means of magnetic fields. Recently, the application of magnetohydrodynamics in the polymer industry and metallurgy has attracted the attention of many researchers. Several researches investigated the MHD flow [16]–[22].

Majority of the studies are restricted to boundary layer flow and heat transfer in Newtonian fluids. However, due to the increasing importance of nanofluids in recent years a great attention has been given to the study of convective transport of nanofluids together with the magnetohydrodynamics. In addition to this the unsteady flow of nanofluids with a non uniform heat source/sink has been given less attention. Therefore, the aim of the present paper is to study the unsteady magnetohydrodynamic flow and heat transfer of nanofluids over stretching sheet with non uniform heat source/sink. The combined effect of all the above mentioned parameters has not been reported so far in the literature, which makes the present paper unique.

The governing highly nonlinear partial differential equation of momentum, energy and concentration fields have been simplified by using suitable similarity transformations and then solved numerically with the help of a powerful, easy to use method called the Keller box method. This method has already been successfully applied to several non linear problems corresponding to parabolic partial differential equations. As discussed in [23] the exact discrete calculus associated with the Keller-Box Scheme is shown to be fundamentally different from all other mimic numerical methods. The box-scheme of Keller is basically a mixed finite volume method, which consists in taking the average of a conservation law and of the associated constitutive law at the level of the same mesh cell.

II. Mathematical Formulation

Consider a two-dimensional unsteady laminar boundary layer flow of nanofluids over a continuously stretching sheet. At time $t = 0$, the plate is impulsively stretched with a velocity $U_w(x,t) = {bx}/{1-at}$ where a and b are positive constants. If we consider the Cartesian coordinate system with the origin fixed in such a way that, the x-axis is taken along the direction of the continuous stretching surface and the y-axis is measured normal to the surface of the sheet as shown schematically in Fig. 1. The fluid is electrically conducting under the influence of an applied magnetic field $B(x)$ normal to the stretching surface. Since the magnetic Reynolds number is very small for most fluid used in industrial applications it is assumed that the induced magnetic field is negligible in comparison to the applied magnetic field. The fluid is a water based nanofluid containing two different types of nanoparticles; Alumina and copper nanoparticles. It is assumed that the base fluid and the nanoparticles are in thermal equilibrium and no slip occurs between them. The nanofluid motion is caused solely by the stretching of the sheet. The surface is assumed to have a non-uniform internal heat generation/absorption and the surface temperature and concentration varies with the coordinate x and time t. The thermophysical properties of the nanofluid are given in Table I (see Oztop and Abu-Nada [24]).

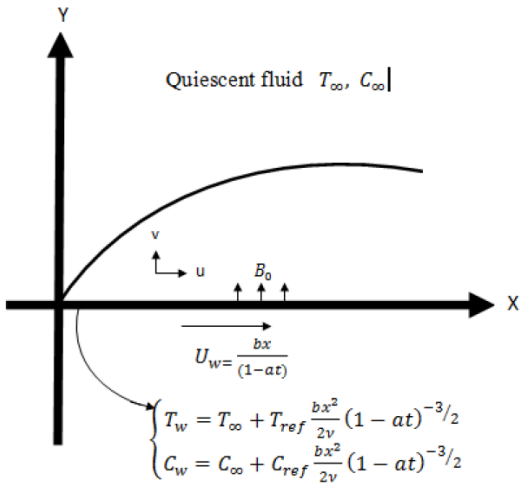

Fig. 1 Physical flow model

The governing equations under unsteady condition are represented by:

$$\frac{\partial u}{\partial x} + \frac{\partial v}{\partial y} = 0 \tag{1}$$

$$\frac{\partial u}{\partial t} + u\frac{\partial u}{\partial x} + v\frac{\partial u}{\partial y} = \frac{\mu_{nf}}{\rho_{nf}}\frac{\partial^2 u}{\partial y^2} - \frac{\sigma B^2(x)}{\rho_{nf}}u \tag{2}$$

$$\frac{\partial T}{\partial t}+u\frac{\partial T}{\partial x}+v\frac{\partial T}{\partial y}=\alpha_{nf}\frac{\partial^2 T}{\partial y^2}+\frac{1}{(\rho c_p)_{nf}}q''' \quad (3)$$

$$\frac{\partial C}{\partial t}+u\frac{\partial C}{\partial x}+v\frac{\partial C}{\partial y}=D\frac{\partial^2 C}{\partial y^2}+ \quad (4)$$

where t is the time, u and v are the velocity components in the x and y directions respectively. T and C are the temperature and concentration of the nanofluid, respectively. B is the uniform magnetic field strength, σ is the electrical conductivity, c_p is the specific heat at constant pressure, D is the species diffusivity, q''' is the non uniform heat generated (>0) or absorbed (<0) per unit volume. μ_{nf}, ρ_{nf}, α_{nf}, and $(\rho c_p)_{nf}$ are the dynamic viscosity, density, thermal diffusivity, and heat capacitance of the nanofluid, respectively, which are given as [25], [26]:

$$\nu_f=\frac{\mu_f}{\rho_f},\ \rho_{nf}=(1-\phi)\rho_f+\phi\rho_s,$$

$$\alpha_{nf}=\frac{k_{nf}}{(\rho c_p)_{nf}},\quad \mu_{nf}=\frac{\mu_f}{(1-\phi)^{2.5}},$$

$$(\rho c_p)_{nf}=(1-\phi)(\rho c_p)_f+\phi(\rho c_p)_s,$$

$$\frac{k_{nf}}{k_f}=\frac{(k_s+2k_f)-2\phi(k_f-k_s)}{(k_s+2k_f)+\phi(k_f-k_s)} \quad (5)$$

In which $\nu_f, \mu_f, \rho_f, k_f$ are the kinematic viscosity, dynamic viscosity, density, and thermal conductivity of the base fluid respectively. ρ_s,k_s, $(\rho c_p)_s$ are the density, thermal conductivity, and heat capacitance of the nanoparticle respectively; ϕ is the solid volume fraction of nanoparticles and k_{nf} is thermal conductivity of the nanofluid.

The value of q''' is chosen approximately as in Abo-Eldahab and Aziz [27].

$$q'''=\frac{k_{nf}U_w}{xv_f}[A^*(T_w-T_\infty)e^{-\eta}+B^*(T-T_\infty)] \quad (6)$$

where $A^*$and B^* are parameters of space dependent and temperature dependent heat generation/absorbtion. It is noted that both $A^*$and B^* are positive to internal heat source and negative to internal heat sink.

The associated boundary conditions to the flow problem can be written as

$$\left.\begin{matrix} u=U_w=\frac{bx}{1-at} \\ T=T_w=T_\infty+T_{ref}\frac{bx^2}{2v_f}(1-at)^2 \\ C=C_w=C_\infty+C_{ref}\frac{bx^2}{2v_f}(1-at)^2 \end{matrix}\right\}\ \text{at}\ y=0$$

$$u\longrightarrow 0, T\longrightarrow T_\infty, C\longrightarrow C_\infty\ \text{as}\ y\longrightarrow\infty \quad (7)$$

In which a and b are constants. T_w and C_w are the temperatures and concentration of the sheet, respectively. T_{ref} and C_{ref} are constant reference temperature and concentration, respectively. T_∞ and C_∞ are the temperature and concentration of the nanofluid far away from the sheet, respectively. In this study, the sheet is assumed to be heated and its temperature and concentration is higher compared to the free stream temperature $T_\infty$and concentration, C_∞

To obtain similarity transformation, it is assumed that the magnetic field $B(x)$ is of the form:

$$B(x)=\frac{B_0}{\sqrt{1-at}}$$

where B_0 is the constant magnetic field.

Introducing the following similarity transformations

$$\eta=y\sqrt{\frac{b}{\nu_f(1-at)}},\ u=\frac{bx}{1-at}f'(\eta),\qquad v=-\sqrt{\frac{b\nu_f}{(1-at)}}f(\eta),$$

$$\theta(\eta)=\frac{T-T_\infty}{T_w-T_\infty},\ \ \mathrm{h}(\eta)=\frac{C-C_\infty}{C_w-C_\infty} \quad (8)$$

Making use of (8), the continuity (1) is automatically satisfied and (2)-(4) and (7) reduces to

$$f'''+\phi_1\left[ff''-f'^2-S(f'+\frac{1}{2}\eta f'')-\frac{M}{\phi_2}f'\right]=0 \quad (9)$$

$$\theta''+\phi_3 Pr\frac{k_f}{k_{nf}}\left[f\theta'-\frac{1}{2}S(3\theta+\eta\theta')\right]+A^*e^{-\eta}+B^*\theta=0 \quad (10)$$

$$\mathrm{h}''+Le(f\mathrm{h}'-2f'h-\frac{1}{2}S(3h+\eta h'))=0 \quad (11)$$

with boundary conditions

$$f(0)=0, f'(0)=1, \theta(0)=1, h(0)=1,$$

$$f'(\eta)\to 0, \theta(\eta)\to 0, h(\eta)\to 0, \text{as}\ \eta\to\infty \quad (12)$$

where $f(\eta)$, $\theta(\eta)$ and $h(\eta)$ are the dimensionless velocity, temperature and nanoparticle concentration, respectively, primes denote differentiation with respect to the similarity variable $\eta.S=\frac{a}{b}, M=\frac{\sigma B_0^2}{\rho_f b}, Pr=\frac{\nu_f(\rho c_p)_f}{k_f}$ and $Sc=\frac{\nu_f}{D}$ represent the unsteadiness parameter, magnetic parameter, Prandtl number and Schmidt number, respectively and the constants ϕ_1, ϕ_2 and ϕ_3 that depend on the nanoparticle volume fraction are given by

$$\phi_1=(1-\phi)^{2.5}\left(1-\phi+\phi\frac{\rho_s}{\rho_f}\right),$$

$$\phi_2=1-\phi+\phi\frac{\rho_s}{\rho_f},$$

$$\phi_3=1-\phi+\phi\frac{(\rho c_p)_s}{(\rho c_p)_f} \quad (13)$$

The physical quantities of interest in this problem are the local skin friction coefficient C_f, the Nusselt number Nu_x, which represents the rate of heat transfer at the surface of the plate and the local Sherwood number Sh_x, which represents

the rate of mass transfer at the surface of the plate, which are defined as

$$C_f = \frac{2\tau_w}{\rho_f U_w^2}, Nu_x = \frac{xq_w}{k_f(T_w - T_\infty)}, Sh_x = \frac{xJ_w}{D(C_w - C_\infty)} \quad (14)$$

where τ_w is the skin friction, q_w is the heat flux and J_w is the mass flux through the plate, which are given by

$$\tau_w = -\mu_{nf}\left(\frac{\partial u}{\partial y}\right)_{y=0}$$

$$q_w = -k_{nf}\left(\frac{\partial T}{\partial y}\right)_{y=0}$$

$$J_w = -D\left(\frac{\partial C}{\partial y}\right)_{y=0} \quad (15)$$

Making use of (8) and (5) in (14), the dimensionless skin friction coefficient, wall heat and mass transfer rates are obtained as

$$C_f(1-\phi)^{2.5}\sqrt{Re_x} = -2f''(0),$$

$$\frac{Nu_x}{\sqrt{Re_x}}\frac{k_f}{k_{nf}} = -\theta'(0)$$

$$\frac{Sh_x}{\sqrt{Re_x}} = -h'(0) \quad (16)$$

where $Re_x = \frac{xU_w}{\nu_f}$ is the local Reynolds number.

III. Numerical Solutions

The system of non linear ordinary differential equations (9) - 11) together with the boundary condition (12) were solved numerically using a very efficient finite difference scheme known as Keller box method. The scheme employed is the box method developed by Keller [23]. This method has been shown to be particularly accurate for parabolic problems. It is much faster, easier to program and it is chosen because it seems to be the most flexible of the common methods, being easily adaptable to solving equations of any order. The Keller-box method is essentially an implicit finite difference scheme, which has been found to be very suitable in dealing with nonlinear problems. Details of the method may be found in many recent publications, and here we have used the procedure outlined in Cebeci and Pradshaw [28].

One of the basic ideas of the box method is to write the governing system of equations in the form of a first order system. First derivatives of u and other quantities with respect to η must therefore be introduced as new unknown functions. With the resulting first order equations, the "centered-difference" derivatives and averages at the midpoints of net rectangles and net segments are used, as they are required to get accurate finite difference equations. The resulting finite difference equations are implicit and nonlinear. Newton's method is first introduced to linearize the nonlinear system of equations before a block-tridiagonal factorization scheme is employed on the coefficient matrix of the finite difference equations. The solution of the linearized system of difference equations can be obtained in a very efficient manner by using the block-elimination method [28]. In this study a uniform grid of size $\Delta\eta = 0.01$ is chosen to satisfy the convergence criteria of 10^{-6}, which gives about a four decimal places accuracy for most of the prescribed quantities.

IV. Results and Discussion

We have studied heat and mass transfer in nanofluids unsteady flow due to a stretching sheet with non-uniform heat source/sink. We considered two different types of nanoparticles, namely, Alumina and Copper, with water as the base fluid (i.e. with a constant Prandtl number Pr = 6.2). The thermophysical properties of the nanofluids were assumed to be functions of the volume fraction. The transformed non linear equations (9) - (11) subjected to the boundary condition (12) was solved numerically using Keller box method, which is described in Cebeci and Bradshaw [28]. The velocity, temperature, and concentration profiles were obtained and utilized to compute the skin-friction coefficient, the local Nusselt number, and local Sherwood number in (16). The numerical results for different values of the governing parameters viz., nanoparticle volume fraction ϕ, unsteadiness parameter S, magnetic field parameter M, Schmidt number Sc, space-dependent parameter A^* and temperature-dependent parameter B^* for heat source/sink are presented in graphs. In the absence of nanoparticles, to validate the accuracy of our results a comparison has been made with previously reported works in the literature. The comparisons are found to be in an excellent agreement (see Tables II and III).

The skin friction coefficients for different values of the magnetic parameter M are given in Table II. It can be seen from Table II that the magnitude of $f''(0)$ increases with an increase in M. Increasing values of M resulted in a considerable opposition to the flow due to a Lorenz drag force which causes the values of skin friction coefficient to increase. Moreover, the comparison of the results with the exact solution (17) and ADM-Pade [29] revealed a good agreement.

$$f(\eta) = \frac{1-e^{-\sqrt{1+M}\eta}}{\sqrt{1+M}},\ f''(0) = -\sqrt{1+M} \quad (17)$$

The heat transfer coefficients are shown in Table III for different values of the Prandtl number Pr and the temperature-dependent parameter B^* for heat source/sink. It can be observed that the rate of heat transfer increases with increasing values of Pr and decreasing values of B^*. The present results showed a good agreement with the earlier findings by Vajravelu and Ropper [30] and Tsai et al. [3].

TABLE I
THERMOPHYSICAL PROPERTIES OF BASE FLUID AND NANOPARTICLES

Physical properties	Water	Cu	Al_2O_3
$\rho(Kg\,m^{-3})$	997.1	8933	3970
$c_p(J\,Kg\,K^{-1})$	4179	385	765
K($Wm^{-1}K^{-1}$)	0.613	400	40

TABLE II
COMPARISON OF THE SKIN FRICTION COEFFICIENT – $f''(0)$ FOR DIFFERENT VALUES OF M, WHEN $\Phi = S = 0$

M	[29]	Exact	Present study
1	1.41421	1.41421	1.4142
5	2.44948	2.44948	2.4495
10	3.31662	3.31662	3.3166

TABLE III
COMPARISON OF THE WALL HEAT TRANSFER – $\theta'(0)$ FOR VARIOUS VALUES OF B^*, WHEN $\Phi = S = M = A^* = 0$

B^*	Pr	[30]	[3]	Present study
-1	1	1.710937	1710937	1.7109
-2	2	2.486000	2.485997	2.4860
-3	3	3.028179	3.028177	3.0822
-4	4	3.585194	3.585192	3.5852
-5	5	4.028535	4.028540	4.0286

The following figures show a comparison on the flow, heat and mass transfer characteristics between the Al_2O_3- water nanofluid (plotted by solid lines) and Cu-water nanofluid (plotted by dashed lines).

Fig. 2 shows, the velocity distribution in the entire flow of the Al_2O_3- waterand $Cu-$ water nanofluids. It is noted that the velocity is maximum near the plate surface but decreases gradually to zero at the free stream far away from the plate satisfying the boundary conditions. It also shows that $Cu-$ water nanofluid attains zero free stream velocity faster with a smaller momentum boundary layer thickness as compared to Al_2O_3- water nanofluid.

The effect of unsteadiness parameter S on the velocity, temperature and concentration profiles in the case of the Al_2O_3- water and $Cu-$ water nanofluids are depicted in Figs. 3, 4, 5, respectively. It is observed that the velocity, temperature and concentration profiles decrease with an increase in S for both types of nanofluids. From Fig. 3, it can be observed that the velocity distribution and the velocity boundary layer thickness are higher in the Al_2O_3- water nanofluids than in the $Cu-$ water nanofluid. While the temperature and concentration profiles and boundary layer thicknesses are higher in the $Cu-$ water nanofluid than in the Al_2O_3- water nanofluid (See Figs. 4 and 5).

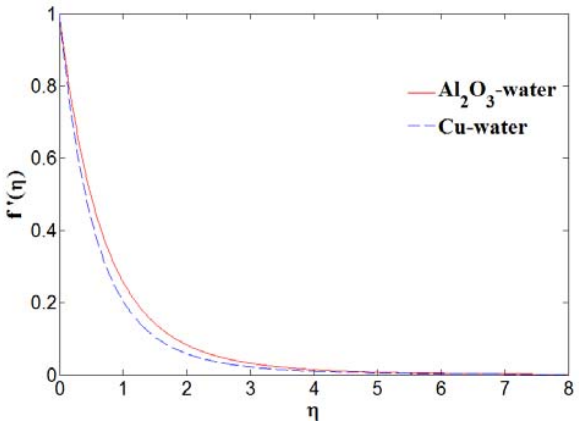

Fig. 2 Velocity distribution $f'(\eta)$of Al_2O_3-water and $Cu-$water nanofluids, when $\phi = 0.2,\ M = S = 1, Pr = 6.2, A^* = B^* = 0.05, Sc = 1$

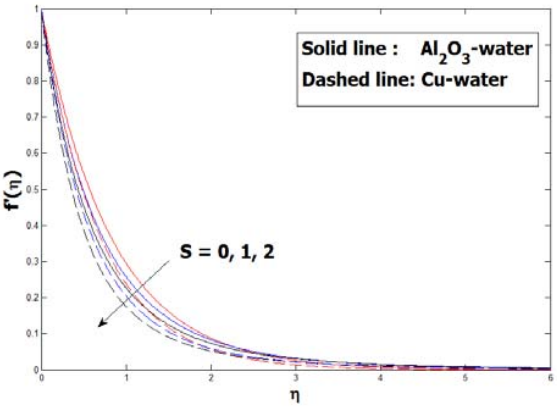

Fig. 3 Effects of S on the velocity distribution $f'(\eta)$, when $\phi = 0.2$, $M = 1, Pr = 6.2, A^* = B^* = 0.05, Sc = 1$ in case of Al_2O_3-water and $Cu-$water nanofluids

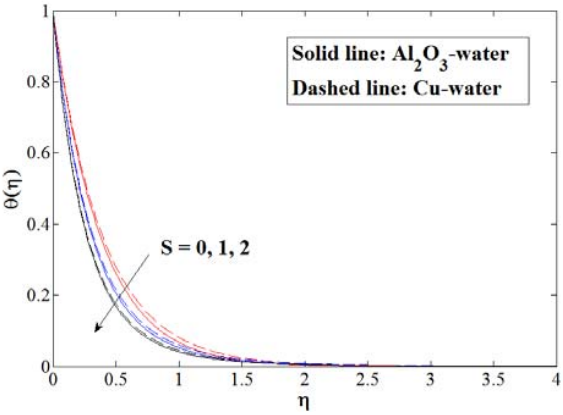

Fig. 4 Effects of S on the temperature distribution $\theta(\eta)$, when $\phi = 0.2,\ M = 1, Pr = 6.2, A^* = B^* = 0.05, Sc = 1$ in case of Al_2O_3-water and $Cu-$water nanofluids

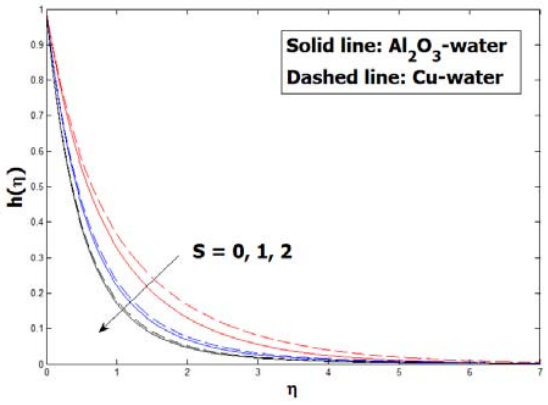

Fig. 5 Effects of S on the concentration profile $h(\eta)$, when $\phi = 0.2$, $M = 1, Pr = 6.2, A^* = B^* = 0.05, Sc = 1$ in case of Al_2O_3 −water and Cu −water nanofluids.

Figs. 6 and 7, present the effect of the spaced dependent and temperature dependent heat source/sink parameters A^* and B^*, respectively, on the temperature profile for both the Al_2O_3 − water and Cu − water nanofluids. Fig. 6 illustrates, that the temperature profile increases with increasing values of A^*. This is because, with an increase in the value of $A^* > 0$ (heat source), the boundary layer generates energy which causes the temperature profile to increase. Where as in the case of $A^* < 0$ (absorbtion), the boundary layer absorbs energy causing the temperature of the nanofluid to fall considerably with decreasing values of $A^* < 0$. It can also be observed that the temperature profile is slightly higher in the Al_2O_3 − water nanofluid than in the Cu − water nanofluid.

Fig. 7 demonstrates that, the temperature profile increases with increasing the values of the temperature dependent heat source/sink parameter B^*, in both the Al_2O_3 − water and Cu − water nanofluids. Thus energy is released when $B^* > 0$ which causes the temperature of the fluid to increase, whereas when the energy is absorbed by decreasing the values of $B^* < 0$, the temperature drops significantly near the boundary layer. Moreover the temperature drops slightly faster in the Cu − water than in the Al_2O_3 − water nanofluid with decreasing the values of B^*.

Fig. 8 shows, the effect of the Schmidt number Sc on the concentration profile. It is noted that the concentration profile decreases with an increase in the value of Sc for both the Al_2O_3 − water and Cu − water nanofluids. This is due to the decrease in the decrease in the solutal boundary layer thickness. Moreover, the concentration boundary layer thickness of the Cu − water nanofluid is thicker than the Al_2O_3 − water nanofluid.

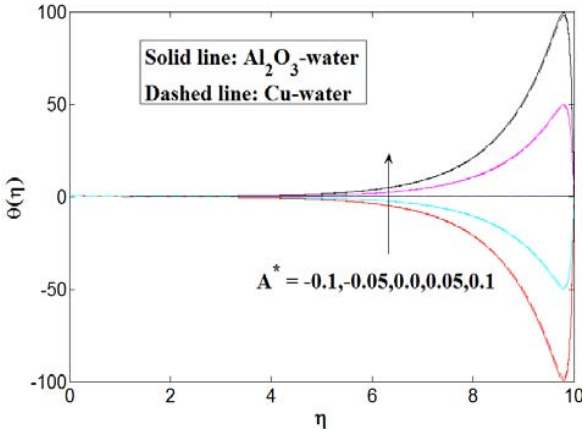

Fig. 6 Effects of A^* on the temperature distribution $\theta(\eta)$, when $\phi = 0.2,\ M = S = 1, Pr = 6.2, B^* = 0.05, Sc = 1$ in case of Al_2O_3 −water and Cu −water nanofluids

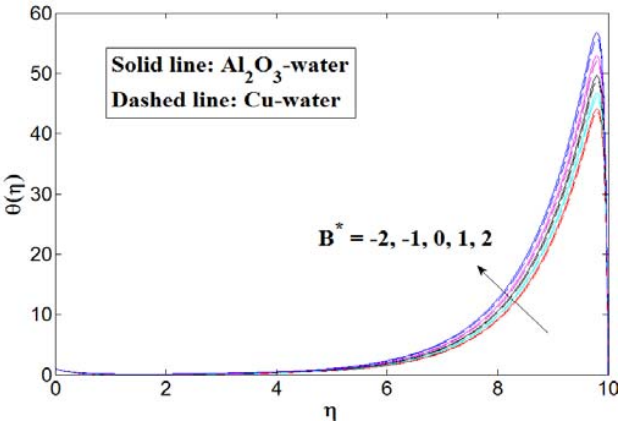

Fig. 7 Effects of B^* on the temperature distribution $\theta(\eta)$, when $\phi = 0.2,\ M = S = 1, Pr = 6.2, A^* = 0.05, Sc = 1$ in case of Al_2O_3 −water and Cu −water nanofluids

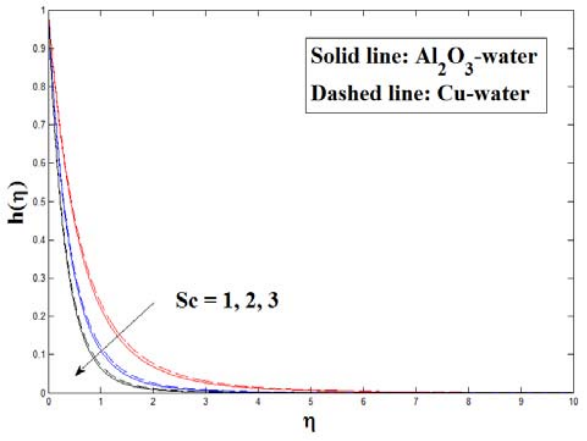

Fig. 8 Effects of Sc on the concentration profile $h(\eta)$, when $\phi = 0.2$, $M = S = 1, Pr = 6.2, A^* = B^* = 0.05$ in case of Al_2O_3 −water and Cu −water nanofluids

Figs. 9-13 illustrate the effects of various parameters on the skin friction, rate of heat and mass transfer at the wall in case of the Al_2O_3- water and Cu-water nanofluids.

Fig. 9 shows, the variation of the wall skin friction coefficient with the nanoparticle volume fraction ϕ for different values of the magnetic parameter M in case of the Al_2O_3- water and $Cu-$ water nanofluids. It is noted that the wall skin friction coefficient is an increasing function of ϕ for $Cu-$ water nanofluid and decreasing function of ϕ for the Al_2O_3- water nanofluid, while the skin friction coefficient increases with an increase in M in both the Al_2O_3- water and $Cu-$ water nanofluids. Moreover, the wall skin friction is higher in the $Cu-$ water nanofluid compared to the Al_2O_3- water nanofluid. Thus, the $Cu-$ water nanofluid gives a higher drag force in opposition to the flow as compared to the Al_2O_3- water nanofluid.

Fig. 10, present the effects of the nanoparticle volume fraction ϕ and Magnetic parameter M on the local Nusselt number Nu_x, which is a measure of rate of heat transfer at the wall. It is clear that, the wall heat transfer rate decreases with increasing the nanoparticle volume fraction and magnetic parameter in both Al_2O_3- water and $Cu-$ water nanofluids. In addition to this, the rate of heat transfer at the wall is higher in Al_2O_3- water nanofluid than in $Cu-$ water nanofluid.

The combined effect of the space dependent A^* and temperature dependent B^* heat source/ sink parameters on the wall heat transfer rate is shown in Fig. 11 in case of Al_2O_3- water and $Cu-$ water nanofluids. The rate of heat transfer is a decreasing function of A^* and B^* in both fluids. Moreover, the rate of heat transfer at the wall is less in case of the $Cu-$ water nanofluid compared to the Al_2O_3- water nanofluid.

Figs. 12 and 13 show the variation of mass transfer rate, Sherwood number, with different parameters. Fig. 12 shows, the variation of the mass transfer rate at the plate surface with ϕ for different values of the magnetic parameter M in case of Al_2O_3- water and Cu-water nanofluids. The rate of mass transfer decreases with increasing M and ϕ, while it increase with ϕ in case of Al_2O_3- water nanofluid. The Sherwood number increases with an increase in S and Sc (see Fig. 13). In Figs. 12 and 13, it is observed that the Al_2O_3- water nanofluid has higher rate of mass transfer than the $Cu-$ water nanofluid.

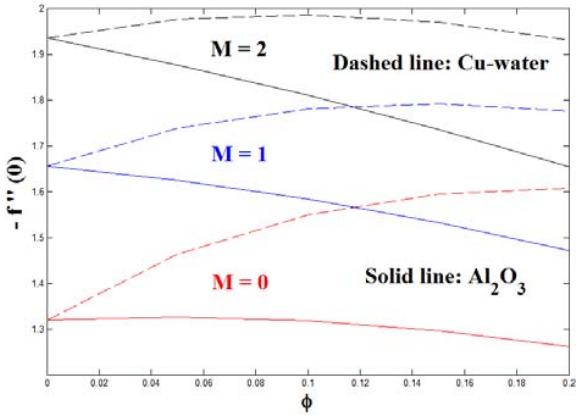

Fig. 9 Variation of the skin friction coefficient $-f''(0)$ with ϕ for different values of M, when $S = 1, Pr = 6.2, A^* = B^* = 0.05, Sc = 1$ in case of Al_2O_3-water and $Cu-$water nanofluids

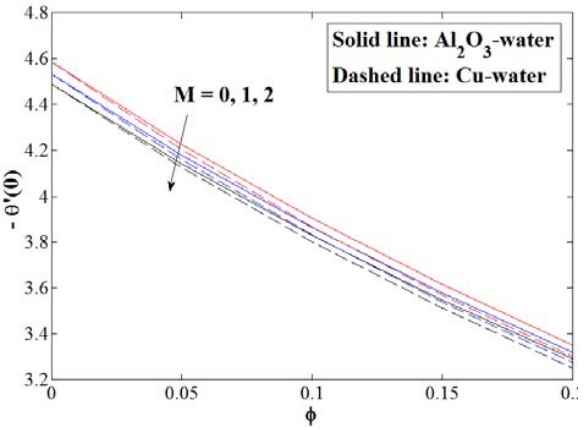

Fig. 10 Variation of the local Nusselt number $-\theta'(0)$ with ϕ for different values of M, when $S = 1, Pr = 6.2, A^* = B^* = 0.05, Sc = 1$ in case of Al_2O_3-water and $Cu-$water nanofluids

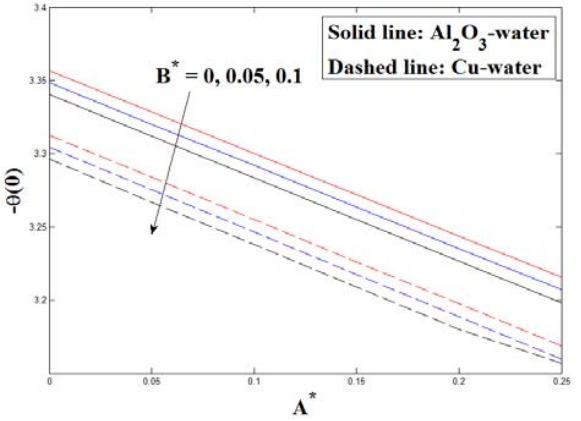

Fig. 11 Variation of the local Nusselt number $-\theta'(0)$ with A^* for different values of B^*, when $\phi = 0.2, M = S = 1, Pr = 6.2, Sc = 1$ in case of Al_2O_3-water and $Cu-$water nanofluids

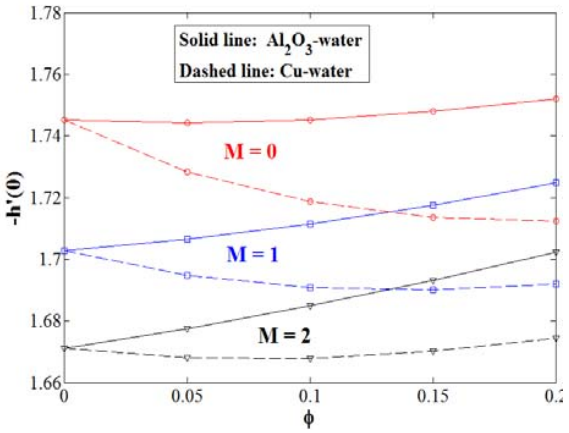

Fig. 12 Variation of the local Sherwood number $-h'(0)$ with ϕ for different values of M, when $S = 1, Pr = 6.2, A^* = B^* = 0.05, Sc = 1$ in case of Al_2O_3 −water and Cu −water nanofluids

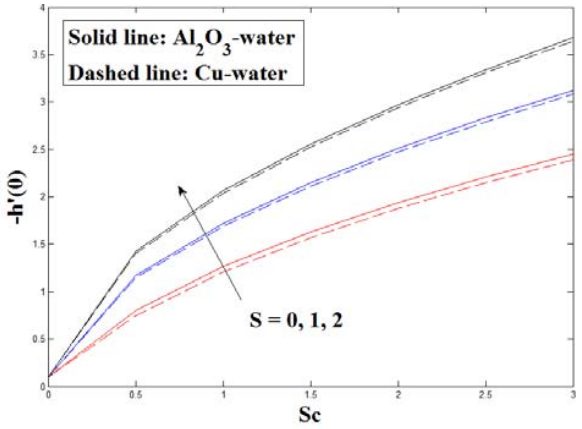

Fig. 13 Variation of the local Sherwood number $-h'(0)$ with Sc for different values of S, when $\phi = 0.2, M = 1, Pr = 6.2, A^* = B^* = 0.05$ in case of Al_2O_3 −water and Cu −water nanofluids

V. Conclusion

The heat and mass transfer in unsteady MHD boundary-layer flow of nanofluids over stretching sheet with a non uniform heat source/sink is investigated numerically for different types of nanoparticles. The governing nonlinear partial differential equations were transformed into ordinary differential equations using the similarity approach and solved numerically using the Keller box method. Two types of nanofluids were considered, Al_2O_3 −water and Cu −water, and our results revealed, among others, the following.

- The velocity distribution increases with increasing S and the Cu −water shows a thinner velocity boundary thickness than Al_2O_3 −water nanofluid. Thus, the Cu −water nanofluid attains its zero velocity faster than Al_2O_3 −water nanofluid. It is also noted that the wall skin friction increases with increasing M.
- The temperature profile increases with increasing A^*, and B^*, while it decreases with increasing S for both Al_2O_3 −water and Cu −water nanofluids.
- The heat transfer rate at the plate surface decreases with increasing ϕ, M, A^* and B^* in both Al_2O_3 −water and Cu −water nanofluids. Higher values of rate of heat transfer are attained when using the Al_2O_3 nanoparticle.
- The concentration profile is observed to decrease with increasing S. Cu −water nanofluid shows a slightly thicker concentration boundary layer thickness than Al_2O_3 −water nanofluid.
- The mass transfer rate at the plate surface increases with increasing S and Sc, and decrease with M and ϕ, while it increase with ϕ in case of Al_2O_3 −water nanofluid. The Al_2O_3 −water nanofluid has higher rate of mass transfer than the Cu −water nanofluid.

A comparison with previously reported data is made and an excellent agreement is noted.

References

[1] C. D. S. Devi, H. S. Takhar, G. Nath, "Unsteady mixed convection flow in stagnation region adjacent to a vertical surface," *Heat Mass Transfer*, 26(1991) 71-79.
[2] E. M. A. Elbashbeshy, M. A. A. Bazid, "Heat transfer over an unsteady stretching surface," *Heat Mass Transfer*, 41(2004) 1-4.
[3] R. Tsai, K. H. Huang, J. S. Huang, "Flow and heat transfer over an unsteady stretching surface with non-uniform heat source," *Int. Commun. Heat Mass Transfer*, 35(2008) 1340-1343.
[4] A. Ishak, Unsteady, "MHD flow and heat transfer over a stretching plate," *J. Appied Sci*. 10(18)(2010) 2127-2131.
[5] K. Sarit, Das SUSC, Yu. Wenhua, T. Pradeep, "Nanofluids Science and Technology," *1 edition, Honboken, NJ, John Wiley & Sons, Inc*, 2007.
[6] W. Yu, D. M. France, J. L. Routbort, and S. U. S. Choi, "Review and Comparison of Nanofluid Thermal Conductivity and Heat Transfer Enhancements," *Heat Transfer Engineering*, 29(5) (2008) 432-460 (1).
[7] H.U. Kang, S.H. Kim, J.M. Oh, "Estimation of thermal conductivity of nanofluid using experimental effective particle volume," *Exp. Heat Transfer* 19 (3) (2006)181–191.
[8] V. Velagapudi, R.K. Konijeti, C.S.K. Aduru, "Empirical correlation to predict thermophysical and heat transfer characteristics of nanofluids," *Therm. Sci*. 12 (2) (2008) 27–37.
[9] V.Y. Rudyak, A.A. Belkin, E.A. Tomilina, "On the thermal conductivity of nanofluids," *Tech. Phys. Lett.* 36 (7) (2010) 660–662.
[10] H. Masuda, A. Ebata, K. Teramae, N. Hishinuma, "Alteration of thermal conductivity and viscosity of liquid by dispersing ultra-fine particles," *Netsu Bussei* 7 (1993) 227–233.
[11] J. Buongiorno, W. Hu, "Nanofluid coolants for advanced nuclear power plants," *Proceedings of ICAPP* 05: May 2005 *Seoul. Sydney: Curran Associates, Inc*, (2005)15-19.
[12] J. Buongiorno, "Convective transport in nanofluids," *ASME J Heat Transf,* 128(2006)240-250.
[13] W. A. Khan, Pop I., "Free convection boundary layer flow past a horizontal flat plate embedded in a porous medium filled with a nanofluid," *Journal of Heat Transfer,* vol. 133(2011)9.
[14] O.D. Makinde, Aziz A., "MHD mixed convection from a vertical plate embedded in a porous medium with a convective boundary condition," *International Journal of Thermal Sciences* 49(2010)1813-1820.
[15] P. Ganesan, G. Palani, "Finite difference analysis of unsteady natural convection MHD flow past an inclined plate with variable surface heat and mass flux," *International Journal of Heat and Mass Transfer,* 47(19-20)(2004) 4449–4457.
[16] K. Jafar, R. Nazar, A. Ishak, I. Pop, "MHD Flow and Heat Transfer Over stretching/shrinking sheets with external magnetic field, viscous dissipation and Joule Effects," *Can. J. Chem. Eng*. 9999 (2011) 1–11.
[17] M.A.A. Hamada, I. Pop, A.I. Md Ismail, "Magnetic field effects on free convection flow of a nanofluid past a vertical semi-infinite flat plate," *Nonlinear Anal. Real World Appl.* 12 (2011) 1338–1346.
[18] A. Beg, A.Y. Bakier, V.R. Prasad, "Numerical study of free convection magnetohydrodynamic heat and mass transfer from a stretching surface to a saturated porous medium with Soret and Dufour effects," *Comput. Mater. Sci.* 46 (2009) 57–65.

[19] A. Ishak, "Unsteady MHD flow and heat transfer over a stretching plate," *J.Applied sci.* 10(18)(2010) 2127-2130.
[20] T. Fang, J. Zhang, S. Yao, "Slip MHD viscous flow over a stretching sheet – an exact solution," *Commun. Nonlinear Sci. Numer. Simul.* 14 (11) (2009) 3731– 3737.
[21] T. Fang, J. Zhang, S. Yao, "Slip magnetohydrodynamic viscous flow over a permeable shrinking sheet," *Chin. Phys. Lett.* 27 (12) (2010)124702.
[22] O. D. Makinde, "Entropy analysis for MHD boundary layer flow and heat transfer over a flat plate with a convective surface boundary condition," *Int. Journal of Exergy,* 10(2)(2012)142-154.
[23] H. B. Keller, "A new difference scheme for parabolic problems. : Numerical solutions of partial differential equations," *II (Hubbard, B. ed.).,New York: Academic Press*, (1971)327–350.
[24] H.F. Oztop, E. Abu-Nada, "Numerical study of natural convection in partially heated rectangular enclosures filled with nanofluids," *Int. J. Heat Fluid Flow* 29 (2008) 1326–1336.
[25] R.K. Tiwari, M.N. Das, "Heat tranfer augmentation in a two – sided lid – driven diffrentially heated square cavity utilizing nanofluids," *Int. J. Heat Mass Transfer* 50 (2007) 2002–2018.
[26] S. Ahmad, A. M. Rohni, I. Pop, 2011, "Blasius and Sakiadis problems in nanofluids," *Acta Mech.* 218 (2011) 195–204.
[27] Abo-Eldahab EM, Aziz MAE, "Blowing/suction effect on hydromagnetic heat transfer by mixed convection from an inclined continuously stretching surface with internal heat generation/absorption," *Intl J. Thermal Sci*. 43 (7)(2004)709-719.
[28] T. Cebeci, P.Pradshaw, "Physical and Computational Aspects of Convective Heat Transfer," *New York:Springer,* 1988.
[29] Hayat T, Hussain Q, Javed T. "The modified decomposition method and pade approximation for the MHD flow over a non-linear stretching sheet," *Nonlinear Anal: Real World Applications,* 10(2)(2009) 966-973.
[30] Vajravelu K, Roper T , "Flow and heat transfer in a second grade fluid over a stretching sheet," *Intl J. Non-Linear Mech.* 34 (6)(1999)1031-1036.